Journal of Inorganic and Organometallic Polymers and Materials (2021) 31:2980–2989
https://doi.org/10.1007/s10904-021-01876-8

Enhanced *E. coli* Capturing Efficacy Over Magnetic Dextrin–Cobalt Sulfide Nanohybrid as a Promising Water Disinfection System

Mohammad Hassan Amini[1] · **Mostafa Hossein Beyki**[2]

Received: 30 November 2020 / Accepted: 1 January 2021 / Published online: 15 January 2021

Abstract
The aim of this research is synthesis of a promising bacterial elimination nanohybrid for water disinfection. Hence dextrin, a carbohydrate polymer composed of linear α-(1,4)-linked D-glucose, is used as an intermediate to prepare Fe_3O_4–dextrin–CoS nanohybrid. At the first step magnetic dextrin was prepared by one step ultrasound assisted route using Fe^{2+} as iron source and dextrin as capping agent. At the second step functional groups of dextrin was employed to trap Co^{2+} ions for decorating CoS at the biosorbent structure through refluxing route. The structure of the magnetic dextrin and nanohybrid was studied by XRD, EDX, FESEM, TGA and zeta potential measurement. EDX and TGA results confirmed that the CoS has been decorated with high density onto magnetite dextrin structure. The prepared nanohybrid has been employed to capture *Escherichia coli* as a sample pathogen from water solution. Effective parameters on bacterial elimination, i.e., pH, contact time, nanohybrid dosage and presence of anions have been studied. Results showed that at pH of 3.5, contact time of 15 min and nanohybrid dosage of 20 mg *E. coli* capturing efficacy was more than 99% which confirmed high efficiency of the nanosystem in bacteria elimination from water solution.

Keywords Bacteria · CoS · Dextrin · *E. coli* · Magnetite composite

1 Introduction

Water is the most essential substance for living things as all life in our planet requires it to continue living. Among the inhabitants of the earth; the mankind require healthier drinking water than other creatures as an appropriate accessibility of healthy water is the fundamental human right [1, 2]. In recent century, contamination of surface and groundwater sources; especially in terms of microbial pollution accelerate as a result of population increase and expansion of human activity. The most important type of the water contaminant is pathogenic bacteria that originated from municipal sewage and agricultural inputs. This phenomena make the reliable access to clean water a major global challenge as a large population around the world have no access to safe water [3, 4]. One of the most widely distributed pathogen in environment includes gram-negative *Escherichia coli* which is prevalent in farm animals and could be considered as a potential water infection agent to evaluate water quality [5, 6]. Up to now several conventional methods have been developed for elimination of the pathogens from water. These methods needed employment of chlorine compounds, ozone and peroxide. Despite good performances of these chemicals, they generate different kinds of carcinogenic byproducts. Antibiotic usage is another useful method but are becoming less efficient especially for antibiotic-resistant strains [7–9]. Thus, development of techniques with better activity profile is a necessary issue for providing healthy water.

In recent decades, development of nanoscience offer some unique opportunities to resolve water quality issue by expanding of antimicrobial nanostructures [10]. Up to now several nanostructures have been developed to respond this challenge. Most effective ones include: zeolite [11], carbon-based compounds [12, 13], alumina [14], silver nanoparticles [15, 16], silica [17, 18] and metal oxides [19–21]. Organic–inorganic nanocomposites are another promising water disinfection materials [22] hence in recent years,

✉ Mohammad Hassan Amini
Amini@ccerci.ac.ir; hassanamini4@gmail.com

Mostafa Hossein Beyki
mhosseinbaki@yahoo.com

[1] Chemistry and Chemical Engineering Research Center of Iran, Tehran, Iran

[2] School of Chemistry, University College of Science, University of Tehran, Tehran, Iran

hybrid composites of polymers have attracted extensive attention for water purification. Polymer composites display better performances respect to each components and present a synergistic effect. Moreover; composite preparation improves the mechanical, chemical and physical properties of polymers [23, 24].

Water disinfection by using natural polymers with life source, biosorption, is still under research and development. This process is a low price and non hazardous technique which uses biodegradable materials. Approximately most employed biopolymers for water remediation have a same basic structure. In other words they possess simple carbohydrate as monomers that linked together and their structure includes carboxyl, hydroxyl and amino groups that can be employed to bind with target compounds [25, 26]. Hence; in this study, dextrin as a low molecular weight carbohydrate polymer composed of linear α-(1,4)-linked D-glucose polymers is used to prepare a three fragment green water disinfection system. In fact dextrin exerts two different roles in the biosorbent structure. At first it acts as a capping agent for inorganic core as well as a substrate for synthesis of outer inorganic fragment. Secondly, hydroxy groups on dextrin structure is responsible for an increase in bacteria capturing efficiency through binding with bacteria lectin [27, 28]. Despite the worthiness of dextrin it is a water soluble polymer hence its handling as a biosorbent is difficult therefore, preparation of dextrin nanocomposite with binary metal oxides increases the chemical stability and adsorption efficiency of it. Among the various metal oxides, iron oxide is one of the most employed fragments of polymer nanocomposite which incorporation of it into biopolymer structure have shown amazing advancement in polymer properties [21, 29]. It is well known that iron oxide composites show the advantages of magnetic separation from suspension, convenient functionalization with other materials to incorporate multiple properties and reduces operating costs [30–32].

Based on the above mentioned merits and as a part of our interest in the synthesis of nanomaterials and investigation of their application in environmental remediation [33] in the present work a three component magnetic nanocomposite, i.e., Fe_3O_4–dextrin–CoS was synthesized and used for water disinfection. At the first step magnetic dextrin was prepared by one step ultrasound assisted route using Fe^{2+} as iron source and dextrin as capping agent. At the second step functional groups of dextrin was employed to trap Co^{2+} ions for decorating CoS at the biosorbent structure through refluxing route. Selection of CoS is based on the fact that organic and inorganic compounds of sulfur exhibit antimicrobial properties. As a result it seems that cobalt sulfide can increases the bacteria removal efficacy since it is believed that bacteria cell wall membrane can be ruptured by CoS leading to death of cell. Prepared magnetic composite was employed for capturing of *E. coli* as sample pathogen. Moreover, effective parameters on capturing efficiency such as pH, contact time and composite dosage were studied and discussed in details.

2 Experimental

2.1 Materials and Instruments

$FeCl_2{\cdot}4H_2O$, $Co(NO_3)_2{\cdot}6H_2O$, ethanol, ethylene glycol (EG), thiourea, sodium hydroxide and dextrin were purchased from Merck (Darmstadt, Germany). Gram-negative *E. coli*, supplied from Institute Pastor, Tehran, Iran. The structure of the nanocomposite was characterized by field emission scanning electron microscopy (FESEM), vibration sample magnetometer (VSM), thermal gravimetric analysis (TGA), zeta potential measurements and powder X-ray diffraction analysis (XRD). VSM was recorded with Lake Shore Model 7400 (Japan) instrument. FESEM was recorded with Sigma VP instrument (Zeiss). A TA-Q-50 instrument was used to collect TGA data. Zeta potentials were measured using Zetasizer Nano ZS90 (Malvern Instruments, UK). A digital pH-meter (model 692, Metrohm, Herisau, Switzerland) was used for pH adjustment. XRD (X'Pert PRO, with Cu Ka radiation at k = 1.540589 Å) was used to investigate the crystallinity of the nanohybrid.

2.2 Synthesis of Fe_3O_4–Dextrin Magnetic Nanoparticles

About 1.0 g of dextrin was dissolved in 100 mL distilled water after stirring for 5 min. Then 5.2 g of $FeCl_2{\cdot}4H_2O$ was dissolved in 50 mL of distilled water and was poured to the dextrin solution under magnetic stirring. After stirring for 10 min 4.0 g of NaOH in 50 mL distilled water was dripped to the mixture under ultrasound irradiation. After 1 h reaction at 60 °C obtained precipitate was filtered, washed with distilled water then dried at 70 °C for 5 h.

2.3 Synthesis of Cobalt Sulfide Coated Magnetic Dextrin

To prepare CoS coated magnetic dextrin, 1.0 g of magnetic dextrin was added in 80 mL of EG and stirred for 15 min at 120 °C and followed with the addition of 1.6 g of $Co(NO_3)_2{\cdot}6H_2O$. After complete dissolution of the salt, 1.8 g of thiourea in 20 mL of water poured into the mixture and refluxed at 140 °C for 90 min. The obtained black product has been collected with external magnetic field and washed with distilled water then dried at 80 °C for 5 h.

2.4 Bacteria Capture Experiment

Bacterial capturing studies were performed in sterilized physiological saline with bacteria concentration of 1.5×10^8 CFU/mL. In a typical run 20 mg of the nanocomposite was dispersed in the 20 mL of bacterial solutions and incubated in a shaker for 15 min. After collection of the magnetic particles from the suspension, 1.0 mL of the supernatant was collected and analyzed via filter membrane method. The same experiments were performed in the absence of nanoparticles and removal percentage (%R) was calculated as follows:

$$\%R = 100 \times \left(CFU_0 – CFU_t\right)/CFU_0 \quad (1)$$

At the above equation CFU_0 (colony forming unite) is initial cell numbers and CFU_t represent the number of colonies in the supernatant after capturing experiment [34, 35]. Capturing protocol is illustrated at Scheme 1.

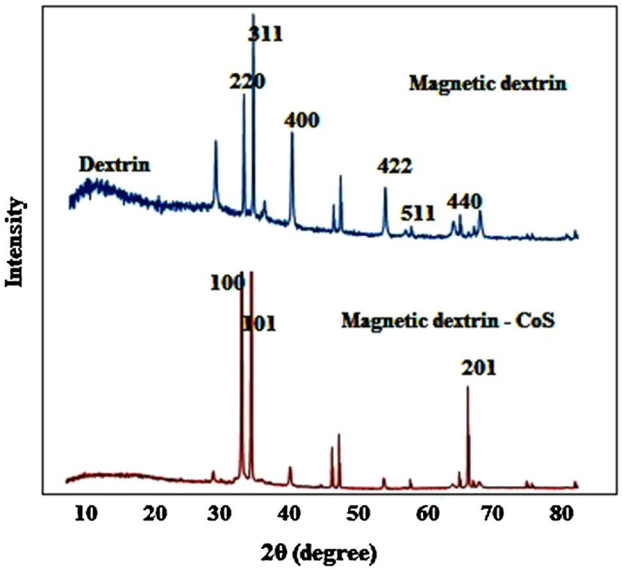

Fig. 1 The XRD pattern of magnetic dextrin and CoS nanocomposite

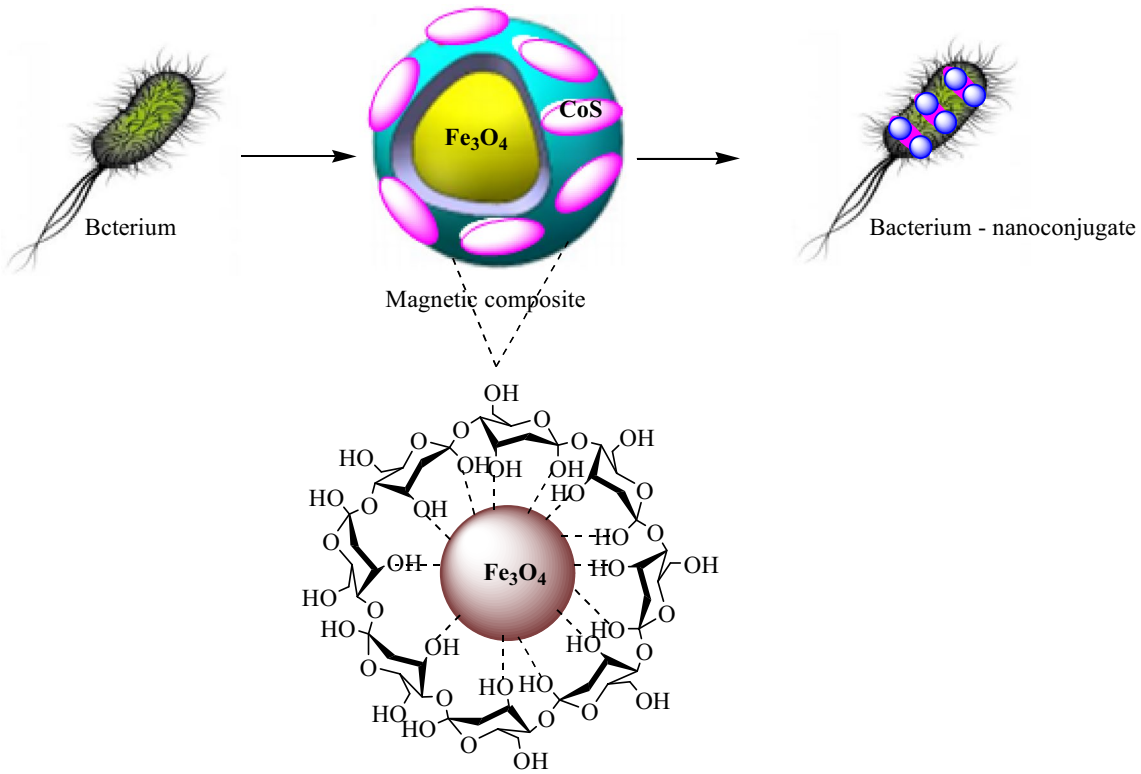

Scheme 1 The protocol for capturing bacteria using CoS nanocomposite

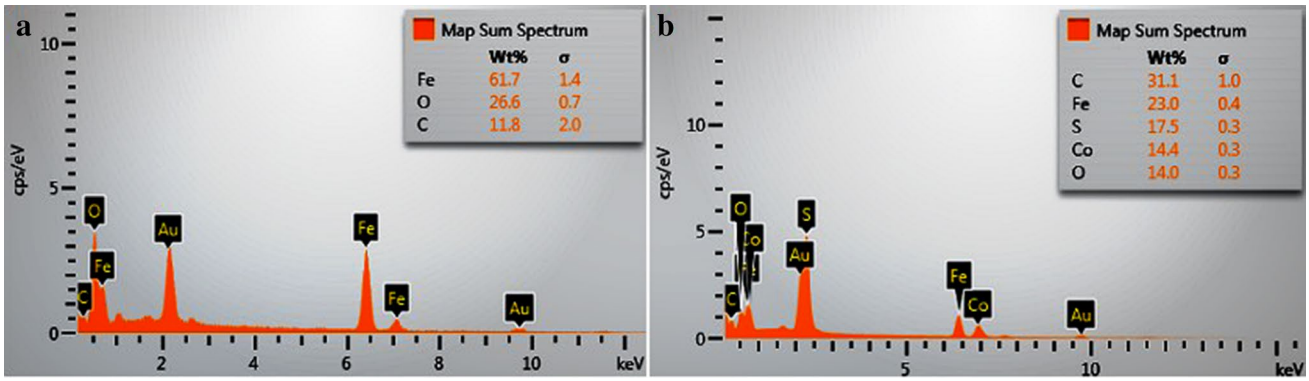

Fig. 2 The EDX spectra of magnetic dextrin (**a**) and CoS nanocomposite (**b**)

3 Results and Discussions

3.1 Characterization

The XRD analysis was used to study the crystallinity of the magnetic dextrin and final nanocomposite and results are shown at Fig. 1. It can be seen that the pattern is dominant with the main peaks of magnetic nanoparticles as the presence of dextrin exerted a low effect on the iron oxide crystallinity. According to the results the Fe_3O_4 show scattering at 2θ° of 30.26, 35.34, 43.22, 53.55, 57.23, and 63.32 corresponding to the (220), (311), (400), (422), (511), and (440) planes that match well with the standard spectra (00-003-0863.CAF). Moreover, one broad peak at around 2θ° of 10 can be assigned to the dextrin [27]. After synthesis of CoS, the pattern showed several new peaks which were assigned to the (100), (101) and (201) planes of cobalt sulfide.

The results of EDX elemental analysis of the magnetic dextrin and the cobalt sulfide composite is illustrated in Fig. 2a, b. According to the results in the spectra all expected component of the nanocomposite are observable as it shows iron, carbon, oxygen, sulfur, and cobalt. Iron, carbon, and oxygen are originated from iron oxide–dextrin structure. Presence of cobalt and sulfur in the EDX spectra is assigned to the cobalt sulfide on the magnetic dextrin surface which confirms the successful synthesis of the nanocomposite.

TGA of the magnetic dextrin and the nanocomposite is shown in Fig. 3. According to the results the graph showed two weight loss stages. First stage occurs in the temperature less than 200 °C. This phenomena can be attributed to the release of the volatile solvent molecule (EG and water) from the material structure. At higher temperatures, another main weight loss has been observed due to the dextrin degradation, which has been accompanied by the release of acetylene, carbon dioxide and hydrogen sulfide. Moreover, it can be seen from TGA profile that magnetic dextrin and composite have shown a total weight loss of

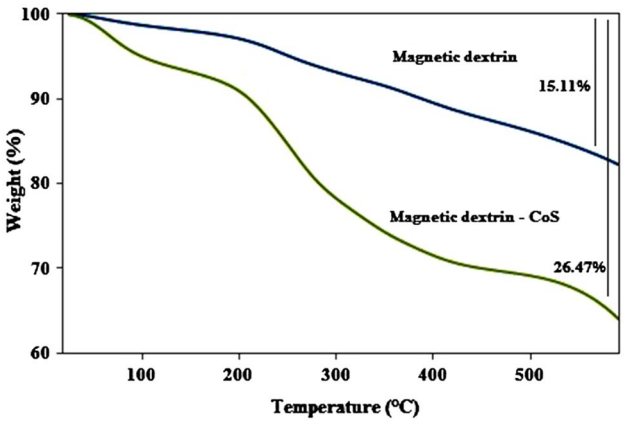

Fig. 3 TGA of the magnetic dextrin and the nanocomposite

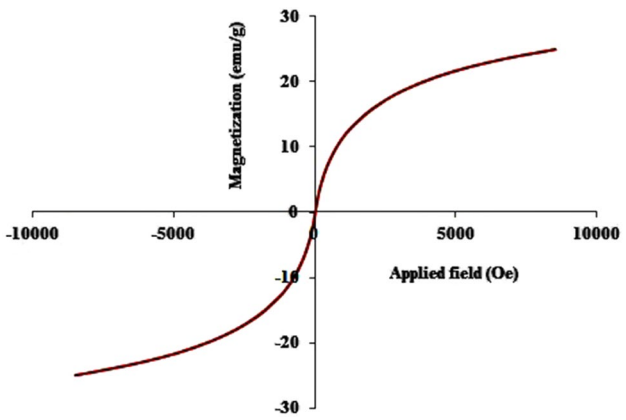

Fig. 4 The VSM graph of magnetic dextrin–CoS nanocomposite

15.11% and 26.47%. As can be seen relative to magnetic dextrin the nanocomposite show higher weight loss which confirmed the immobilization of CoS onto the magnetic dextrin structure.

The magnetic behavior of the nanocomposite was studied by VSM analysis and the hysteresis loop is drowned based on the magnetization versus the applied magnetic field. Results at Fig. 4 showed that the prepared composite possesses a clear hysteresis behavior with the saturation magnetization of 24.8 emu/g. The coercivity and remnant magnetization was 24.9 Oe and 0.6 emu/g, respectively. The value of the magnetic saturation for the synthesized composite is lower than naked magnetite nanoparticles reported in the literature (70 emu/g) [36]. This is owe to the disaffiliation of the dextrin and CoS on the total magnetization as well as a low volume fraction of the iron oxide onto the final composite [37]. The ratio of magnetic remnant to magnetic saturation is 0.024 which lies between 0 and 1 hence, the prepared composite has paramagnetic property [38].

The FESEM images of the magnetic dextrin and the CoS composite is shown at Fig. 5. The image of magnetic dextrin (Fig. 5a) exhibited bundles with an aggregated sphere-like structure which composed of nanoscale particles. After synthesis of cobalt sulfide onto magnetic dextrin structure, agglomerated sheets are formed which combined together. This can be assigned to intramolecular hydrogen bonds of dextrin chain as well as the three dimension growth of cobalt sulfide particles that provide the stiffness of the particles. In other words, the intra- and intermolecular network interaction is the basis of cohesion between the nanocomposite fragments.

3.2 Synthetic Mechanism

For Fe_3O_4 formation simultaneous presence of Fe^{2+} and Fe^{3+} in reaction vessel is necessary. In this research Fe^{2+} was used as the sole iron source to prepare magnetic dextrin with the assistance of ultrasound radiation. In fact sonication generates high temperatures and pressures in the inner environment of the collapsing bubble and bulk solution. This situation converts water into H and OH radicals that accelerates oxidizing of Fe^{2+} ions to Fe^{3+} [39]. At the synthetic process Fe^{2+} precipitates to $Fe(OH)_2$ and due to exposure to O_2 converted to goethite (FeOOH). At the final step $Fe(OH)_2$ and goethite combined together to form Fe_3O_4. The synthetic equations are summarized as follows [40]:

$$FeCl_2 \cdot 4H_2O(s) + 2NaOH(s) \rightarrow Fe(OH)_2(s) + 2NaCl(s) + 4H_2O \quad (2)$$

$$H_2O \rightarrow H\cdot + \cdot OH \quad (3)$$

$$H\cdot + O_2 \rightarrow \cdot OOH \quad (4)$$

$$2 \cdot OOH \rightarrow H_2O_2 + O_2 \quad (5)$$

$$2Fe(OH)_2 + O_2 \rightarrow 2FeOOH + 2H_2O \quad (6)$$

$$Fe(OH)_2 + 2FeOOH \rightarrow Fe_3O_4 + 2H_2O \quad (7)$$

The possible growth mechanism of cobalt sulfide is as follows [41, 42]:

$$Co\left(NO_3\right)_2 \cdot 6H_2O \rightarrow Co^{2+} + 6H_2O + 2NO_3^- \quad (8)$$

$$CH_4N_2S + H_2O \rightarrow 2NH_3 + H_2S + CO_2 \quad (9)$$

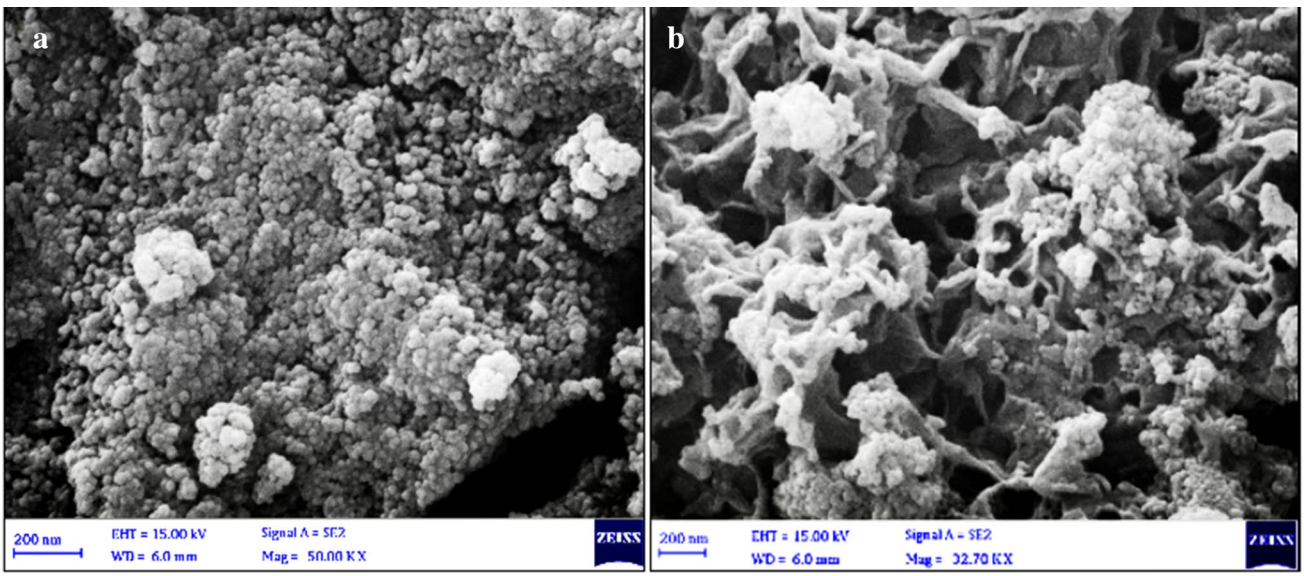

Fig. 5 FESEM image of magnetic dextrin (**a**) and CoS composite (**b**)

$$H_2S + 2H_2O \rightarrow S^{2-} + 2H_3O^+ \quad (10)$$

$$Co^{2+} + S^{2-} \rightarrow CoS \quad (11)$$

The initial stage of reaction includes hydrolysis of the materials and release of the Co^{2+} and S^{2-} ions. The ions reacted to form the CoS particles which grown into aggregated linked structure [43].

3.3 Effect of Time

The sulfur and hydroxyl groups of CoS and magnetic dextrin are responsible for interact with bacteria via attachment to bacterial lectin and the electrostatic attraction [44]. The effect of time was investigated at pH of 5 and *E. coli* concentration of 1.5×10^7 CFU/mL as the amount of composite was 20 mg. The result is shown in Fig. 6a. It can be seen that capturing of bacteria occur efficiently within first 5 min (the efficiency was 90%) and then received to more than 99% after 15 min. For further works the time of 15 min was selected as equilibrium time. To investigate precipitation probability of *E. coli* with increasing time, control tests were also performed. It was found that the *E. coli* densities did not changed hence bacterial sedimentation can be ruled out within the capturing process.

3.4 Effect of Dosage

The effects of CoS nanocomposite dosage on *E. coli* capturing were studied at bacteria concentration of 1.5×10^7 CFU/mL, time of 15 min and pH of 5. Dosage was 10, 20 and 40 mg. According to results at Fig. 6b, with 10 mg nanocomposite, the capture efficiency was 98% after 15 min of reaction. When the dosage increased to 20 mg, the capture efficiencies increased to 99.9%. However, the bacteria removal efficiencies obtained at dosage of 40 mg slightly decreased (99.5%). Lower efficiency at higher dosage may be owing to the screening effect at the outer layer of the composite particles [45] that hinder the binding sites from bacteria cell wall.

3.5 Effect of pH

In this study, the influence of pH on bacterial capturing efficiency was studied in three level of pH including 3.5, 6.5 and 8. The capturing efficiency was calculated as follows:

$$\%R = \left(C_0 - C_e\right) \times 100/C_0 \quad (12)$$

At the equation; R, C_0 and C_e are removal percentage, initial and equilibrium concentrations, respectively.

It was observed in Fig. 7a that capturing efficiency decreased with an increase in pH value. As maximum efficiency were 100% at pH = 3.5 which decreased to 90% at pH = 8. The role of pH on the bacteria removal efficiency can be better described with determining surface charge of the nanocomposite with zeta potential measurement. As can be seen in Fig. 7b, the nanocomposite possesses positive charge at the pH below 4.5. With increasing pH up to 10, the nanocomposites have negative charge hence based on electrostatic attraction it is expected that the nanocomposite has higher capturing efficiency at acidic media. This can be explained from the fact that the cell walls of bacteria have negative charge with isoelectric point of pH 3.5 [46]. In other words adhesion forces are under the influence of pH as with increases of pH, the adhesion forces decreases [47] therefore the efficiency deceases with increase of pH.

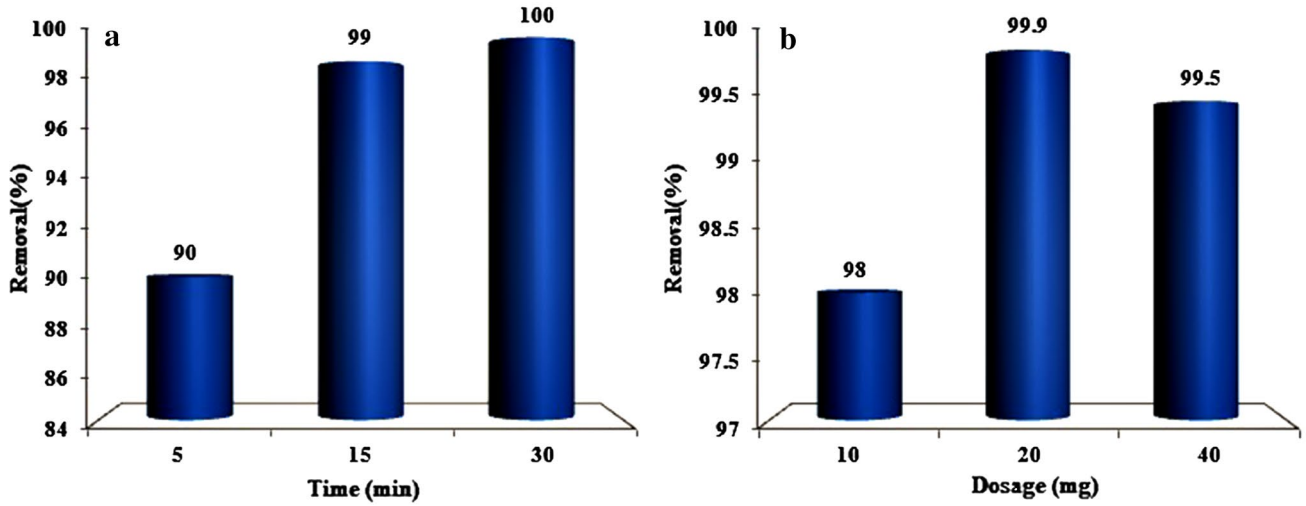

Fig. 6 Effect of time (**a**) and composite dosage (**b**) on *E. coli* capturing

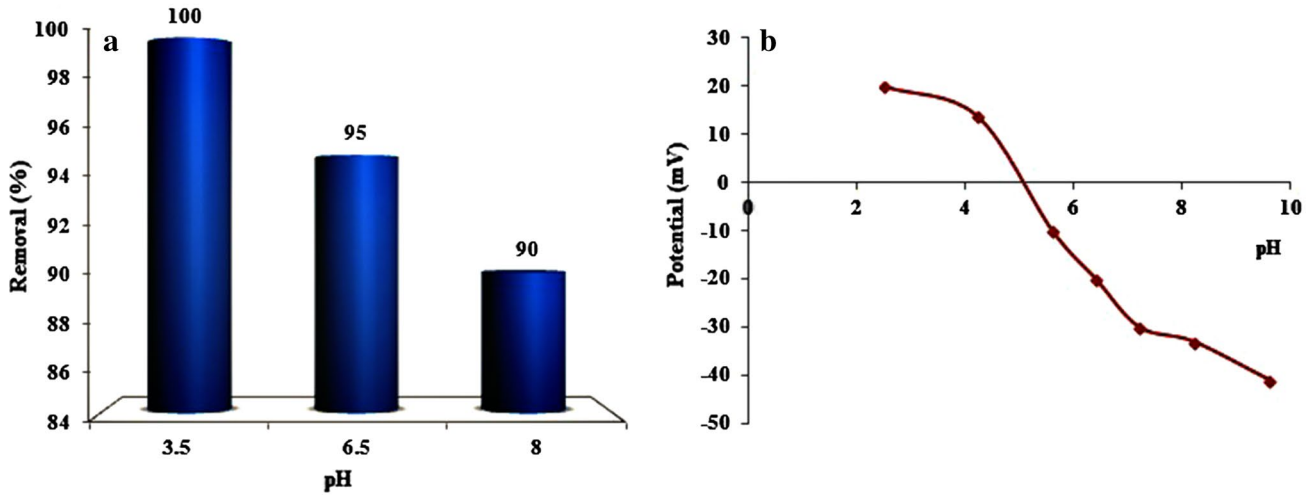

Fig. 7 Effect of pH (**a**) on *E. coli* capturing and zeta potential measurement of the composite (**b**)

According to results at alkali solution the removal percentage is also high (90%). This can be explained with the fact that the composite structure possesses several fragments including Fe_3O_4, polysaccharide and cobalt sulfide. It seems that carbohydrates are good candidates for increase interaction with bacteria lectins [48]. Other reason is binding of highly ionized carboxylate groups on the bacteria surface with Fe ions on the Fe_3O_4 structure through electrostatic interactions [49]. Moreover, hydrogen bonding is another force causes adhesion of nanoparticles on the bacteria cell surfaces [50]. Cobalt sulfide is another main component of the nanocomposite that increases the removal efficacy. It is known that organic and inorganic compounds of sulfur exhibit antimicrobial properties. Hence it is believed that the CoS causes bacteria cell wall membrane rupture and leading to lysis of cell membrane [51].

3.6 Effect of Competitive Anions

E. coli cell wall possesses several functional groups including; hydroxyl, carboxyl, and phosphate groups that are in deprotonated form around pH of 3.5 and higher hence anionic species in the solution may affect the electrostatic interactions between nanoparticles and bacterial cell. To investigate the effect of competitive anions; nitrate, phosphate and sulfate are selected with initial concentration of 10 mM. Other conditions of the experiment were pH = 3.5, time of 20 min and dosage of 15 mg. Results at Fig. 8 showed that in the presence of sulfate and nitrate the capturing efficiencies were more than 99% besides the presence of phosphate reduced the capture efficiency of 99% to around 95%. This is owing to the interaction of phosphate with the functional groups of the composite which reduce the adhesive of bacteria as a result of repulsive energy barriers [52].

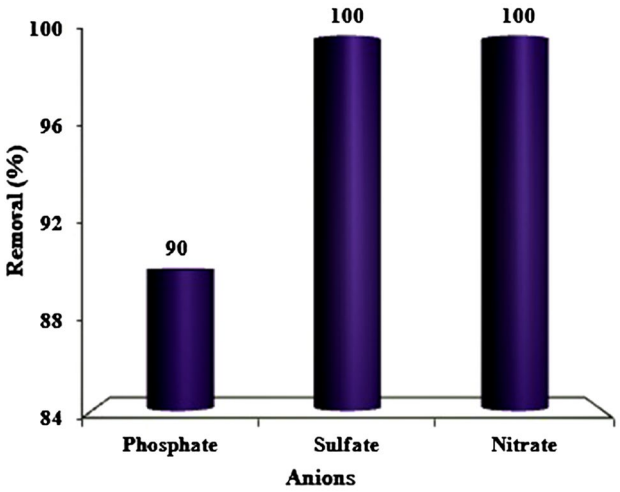

Fig. 8 Effect of anions on the bacteria capturing efficiency

3.7 Recovery and Reuse

Bacteria concentration of 1.5×10^7 CFU/mL and 20 mg of the nanocomposites were used to examine the reuse possibility of material. Ethanol solution (75%) was used as eluent to release the adsorbed bacteria through decomposes of the bacteria cells [7]. Results showed that the capturing efficiencies decreased from more than 99% at first adsorption stage to 95% and 90% after two and three cycle, respectively. This result confirmed that as prepared nanocomposite has good potential to be used as a reusable water disinfection system.

Table 1 Comparing the bacteria capturing performances of the nanocomposite with some reports in literature

Adsorbent	Bacteria	Time (min)	Dosage (mg/mL)	Removal (%)	References
Fe_3O_4@Arginine, Fe_3O_4@Lysine	*E. coli*, *Bacillus subtilis*	20	0.8	>97	[7]
Ag@Fe_2O_3–glucose	*E. coli*	–	0.128	99	[19]
Iron hydroxide-coated sand	*E. coli*	–	–	88	[20]
Fe_3O_4@CTAB	*E. coli*, *B. subtilis*	60	0.5	99	[21]
Ag–Fe_2O_3–fiberglass	*E. coli*	1	0.05	99	[32]
Magnetic glyco-nanoparticles	*E. coli*	45	2	88	[34]
Dextrin–Fe_3O_4–CoS	*E. coli*	15	1	>99	This work

3.8 Comprising Nanocomposite Fragment Performances

To investigate the role of Fe_3O_4, dextrin and CoS on the bacterial capturing, Fe_3O_4 and magnetic dextrin were also employed for *E. coli* removal at pH = 3.5, time of 15 min and dosage of 20 mg. It was found that the removal efficiency was 60% and 80% using magnetite and magnetic dextrin. At the same situation the efficiency was more than 99% by the magnetic dextrin–CoS nanocomposite which confirmed synergism of the components for effective removing of *E. coli*.

The bacteria capturing performances of CoS composite was compared with literature. It can be seen in Table 1 that the capturing efficiency of the nanocomposite is higher than other reports. For example, El-Boubbou et al. [34] used magnetic Glyco-nanoparticles with maximum capturing of 88% after 45 min. Moreover, iron hydroxide-coated sand employed by Park et al. [20] showed 88% *E. coli* capturing. Finally, in comparing with most presented researches, faster equilibrium time and low dosage are other highlights of this work.

4 Conclusions

An effective and reusable water disinfection system was developed based on Fe_3O_4–dextrin–CoS nanohybrid and employed for *E. coli* capturing. Results showed that the magnetic composite have efficiency more than 99% for the pathogen removal. Effect of solution pH on bacteria removal showed that at pH = 3.5, contact time of 15 min and dosage of 20 mg approximately complete removal can be achieved. Moreover, the results confirmed that the nanocomposite has good reusability as after three cycles of experiment the capturing efficiency was more than 90%. Results also confirmed synergism of the nanohybrid components for effective removing of *E. coli* as removal efficiency increased from 60% and 80% using Fe_3O_4 and magnetic dextrin to more than 99% by the magnetic dextrin–CoS nanocomposite.

Acknowledgements The financial support from Chemistry and Chemical Engineering Research Center of Iran is gratefully acknowledged.

Compliance with Ethical Standards

Conflict of interest The authors have no conflicts of interest to declare that are relevant to the content of this article.

References

1. J. Fawell, M.J. Nieuwenhuijsen, Contaminants in drinking water. Br. Med. Bull. **68**, 199–208 (2003). https://doi.org/10.1093/bmb/ldg027
2. Y. Junejo, M. Safdar, M.A. Akhtar, M. Saravanan, H. Anwar, Synthesis of tobramycin stabilized silver nanoparticles and its catalytic and antibacterial activity against pathogenic bacteria. J. Inorg. Organometal. Polym. Mater. **29**, 111–120 (2019). https://doi.org/10.1007/s10904-018-0971-z
3. J. Huang, G. Huang, C. An, X. Xin, X. Chen, Y. Zhao, R. Feng, W. Xiong, Exploring the use of ceramic disk filter coated with Ag/ZnO nanocomposites as an innovative approach for removing Escherichia coli from household drinking water. Chemosphere **245**, 125545 (2020). https://doi.org/10.1016/j.chemosphere.2019.125545
4. S.G. Mulamattathil, C. Bezuidenhout, M. Mbewe, C.N. Ateba, Isolation of environmental bacteria from surface and drinking water in Mafikeng, South Africa, and characterization using their antibiotic resistance profiles. J. Pathog. **2014**, 371208 (2014). https://doi.org/10.1155/2014/371208
5. O. Infections, L.H. Gould, R.K. Mody, P. Clogher, A.B. Cronquist, K.N. Garman, S. Lathrop, C. Medus, N.L. Spina, T.H. Webb, P.L. White, K. Wymore, R.E. Gierke, B.E. Mahon, P.M. Griffin, Increased recognition of non-O157 Shiga toxin-producing Escherichia coli infections in the United States. Foodborne Pathog. Dis. **10**, 453–460 (2013). https://doi.org/10.1089/fpd.2012.1401
6. B.C. Weimer, M.K. Walsh, C. Beer, R. Koka, X. Wang, Solid-phase capture of proteins, spores, and bacteria. Appl. Environ. Microbiol. **67**, 1300–1307 (2001). https://doi.org/10.1128/AEM.67.3.1300
7. Y. Jin, F. Liu, C. Shan, M. Tong, Y. Hou, Efficient bacterial capture with amino acid modified magnetic nanoparticles. Water Res. **50**, 124–134 (2014). https://doi.org/10.1016/j.watres.2013.11.045
8. D. Vo, C. Lee, Antimicrobial sponge prepared by hydrophobically modified chitosan for bacteria removal. Carbohyd. Polym. **187**, 1–7 (2018). https://doi.org/10.1016/j.carbpol.2018.01.082
9. P.Y. Furlan, A.J. Fisher, A.Y. Furlan, M.E. Melcer, D.W. Shinn, J.B. Warren, Magnetically recoverable and reusable nanoparticles

for water disinfection. Invensions **2**, 1–15 (2017). https://doi.org/10.3390/inventions2020010
10. M.J. Meziani, X. Dong, L. Zhu, L.P. Jones, G.E. Lecroy, F. Yang, S. Wang, P. Wang, Y. Zhao, L. Yang, R.A. Tripp, Y.P. Sun, Visible-light-activated bactericidal functions of carbon "quantum" dots. ACS Appl. Mater. Interf. **8**, 10761–10766 (2016). https://doi.org/10.1021/acsami.6b01765
11. M. Zendehdel, B. Shoshtari, Y. Giuseppe, Removal of heavy metals and bacteria from aqueous solution by novel hydroxyapatite/zeolite nanocomposite, preparation, and characterization. J. Iran. Chem. Soc. **13**, 1915–1930 (2016). https://doi.org/10.1007/s13738-016-0908-9
12. J. Liu et al., Yolk/shell nanoparticles: new platforms for nanoreactors, drug delivery and lithium-ion batteries. Chem. Commun. **47**, 12578–12591 (2011)
13. S. Zavareh, E. Norouzi, Impregnation of GO with Cu^{2+} for enhancement of aniline adsorption and antibacterial activity. J. Water Process Eng. **20**, 160–167 (2017). https://doi.org/10.1016/j.jwpe.2017.10.012
14. D. Mu, X. Mu, Z. Xu, Z. Du, G. Chen, Removing Bacillus subtilis from fermentation broth using alumina nanoparticles. Bioresour. Technol. **197**, 508–511 (2015). https://doi.org/10.1016/j.biortech.2015.08.109
15. H.M.M. Ibrahim, M.S. Hassan, Characterization and antimicrobial properties of cotton fabric loaded with green synthesized silver nanoparticles. Carbohyd. Polym. **151**, 841–850 (2016). https://doi.org/10.1016/j.carbpol.2016.05.041
16. S. Haq, K. Ansar, Y. Wajid, R. Muhammad, W. Muhammad, N. Ahmed, M. Imran, S. Nadia, S. Amreen, S. Mahfooz, U. Rehman, B. Khan, Green synthesis of silver oxide nanostructures and investigation of their synergistic effect with moxifloxacin against selected microorganisms. J. Inorg. Organometall. Polym. Mater. (2020). https://doi.org/10.1007/s10904-020-01763-8
17. I. Kheshtzar, M. Ghorbani, M. Pashai, Facile synthesis of smart-aminosilane modified-SnO_2/porous silica nanocomposite for high efficiency removal of lead ions and bacterial inactivation. J. Hazard. Mater. **359**, 19–30 (2018). https://doi.org/10.1016/j.jhazmat.2018.07.028
18. M. Padervand, F. Asgarpour, A. Akbari, B.E. Sis, G. Lammel, Hexagonal core–shell–[SiO_2[–MOYI]Cl–]Ag nanoframeworks for efficient photodegradation of the environmental pollutants and pathogenic bacteria. J. Inorg. Organometall. Polym. Mater. (2019). https://doi.org/10.1007/s10904-019-01095-2
19. Z. Wei, Z. Zhou, M. Yang, C. Lin, Z. Zhao, D. Huang, Z. Chen, J. Gao, Multifunctional Ag@Fe_2O_3 yolk–shell nanoparticles for simultaneous capture, kill, and removal of pathogen. J. Mater. Chem. **21**, 16344 (2011). https://doi.org/10.1039/c1jm13691g
20. J.-A. Park, C.-G. Lee, S.-J. Park, J.-H. Kim, S.-B. Kim, Microbial removal using layered double hydroxides and iron (hydr)oxides immobilized on granular media. Environ. Eng. Res. **15**, 149–156 (2010). https://doi.org/10.4491/eer.2010.15.3.149
21. Y. Jin, J. Deng, J. Liang, C. Shan, M. Tong, Efficient bacteria capture and inactivation by cetyltrimethylammonium bromide modified magnetic nanoparticles. Colloids Surf. B Biointerfaces **136**, 659–665 (2015). https://doi.org/10.1016/j.colsurfb.2015.10.009
22. A. Orsuwan, S. Shankar, L.F. Wang, R. Sothornvit, J.W. Rhim, Preparation of antimicrobial agar/banana powder blend films reinforced with silver nanoparticles. Food Hydrocolloids **60**, 476–485 (2016). https://doi.org/10.1016/j.foodhyd.2016.04.017
23. L. Li, J. Iqbal, Y. Zhu, P. Zhang, W. Chen, A. Bhatnagar, Y. Du, Chitosan/Ag-hydroxyapatite nanocomposite beads as a potential adsorbent for the ef fi cient removal of toxic aquatic pollutants. Int. J. Biol. Macromol. **120**, 1752–1759 (2018). https://doi.org/10.1016/j.ijbiomac.2018.09.190
24. R. Kaveh, H. Alijani, M.H. Beyki, Magnetic polyresorcinol@$CoFe_2O_4$@MnS nanoparticles for adsorption of Pb(II), Ag(I), Cr(VI) and bacteria from water solution. Polym. Bull. **77**, 1893–1911 (2020). https://doi.org/10.1007/s00289-019-02835-7
25. M. Hossein Beyki, S. Ehteshamzadeh, S. Minaeian, F. Shemirani, Clean approach to synthesis of graphene like $CuFe_2O_4$ @ polysaccharide resin nanohybrid: Bifunctional compound for dye adsorption and bacterial capturing. Carbohyd. Polym. **174**, 128–136 (2017). https://doi.org/10.1016/j.carbpol.2017.06.056
26. M. Hossein Beyki, H. Alijani, Y. Fazli, Biosorption of aqueous lead and nickel by solvent-free synthesized flake-like polysaccharide resin. Desal. Water Treatm. **3994**, 1–10 (2016). https://doi.org/10.1080/19443994.2016.1173596
27. A. Mittal, R. Ahmad, I. Hasan, Iron oxide-impregnated dextrin nanocomposite: synthesis and its application for the biosorption of Cr(VI) ions from aqueous solution. Desal. Water Treatm. **57**, 15133–15145 (2016). https://doi.org/10.1080/19443994.2015.1070764
28. S. Perret, C. Sabin, C. Dumon, M. Pokorná, C. Gautier, O. Galanina, S. Ilia, N. Bovin, M. Nicaise, M. Desmadril, N. Gilboa-Garber, M. Wimmerová, E.P. Mitchell, A. Imberty, Structural basis for the interaction between human milk oligosaccharides and the bacterial lectin PA-IIL of Pseudomonas aeruginosa. Biochem. J. **389**, 325–332 (2005). https://doi.org/10.1042/BJ20050079
29. S.I. Siddiqui, S.A. Chaudhry, Nigella sativa plant based nanocomposite-$MnFe_2O_4$/BC: an antibacterial material for water purification. J. Clean. Prod. **200**, 996–1008 (2018). https://doi.org/10.1016/j.jclepro.2018.07.300
30. F. Zhang, Z. Wu, Y. Huang, A.A. Keller, Successive removal of E. coli and a mixture of Pb^{2+} and malachite green from water via magnetic iron oxide/phosphate nanocomposites. Colloids Surf. A **578**, 123598 (2019). https://doi.org/10.1016/j.colsurfa.2019.123598
31. J. Kumar, S. Kumar, M. Mishra, H. Sahoo, Amine functionalized magnetic iron oxide nanoparticles: synthesis, antibacterial activity and rapid removal of Congo red dye. J Mol. Liq. **282**, 428–440 (2019). https://doi.org/10.1016/j.molliq.2019.03.033
32. G. Nangmenyi, X. Li, S. Mehrabi, E. Mintz, J. Economy, Silver-modified iron oxide nanoparticle impregnated fiberglass for disinfection of bacteria and viruses in water. Mater. Lett. **65**, 1191–1193 (2011). https://doi.org/10.1016/j.matlet.2011.01.042
33. M. Ghanbarian, R. Nabizadeh, S. Nasseri, F. Shemirani, A.H. Mahvi, M.H. Beyki, A. Mesdaghinia, Potential of amino-riched nano-structured $MnFe_2O_4$@cellulose to biosorption of toxic Cr (VI): modeling, kinetic, equilibrium and comparing studies. Int. J. Biol. Macromol. **104**, 465–480 (2017). https://doi.org/10.1016/j.ijbiomac.2017.06.060
34. K. El-Boubbou, C. Gruden, X. Huang, Magnetic glyco-nanoparticles: a unique tool for rapid pathogen detection, de-contamination and strain differentiation supporting information Kheireddine El-Boubbou. J. Am. Chem. Soc. **129**, 1–26 (2007). https://doi.org/10.1021/ja076086e
35. S. Zhan, Y. Yang, Z. Shen, J. Shan, Y. Li, S. Yang, D. Zhu, Efficient removal of pathogenic bacteria and viruses by multifunctional amine-modified magnetic nanoparticles. J. Hazard. Mater. **274**, 115–123 (2014). https://doi.org/10.1016/j.jhazmat.2014.03.067
36. M.H. Beyki, J. Malakootikhah, F. Shemirani, S. Minaeian, Magnetic $CoFe_2O_4$ @ melamine based hyper-crosslinked polymer: a multivalent dendronized nanostructure for fast bacteria capturing from real samples. Process Saf. Environ. Prot. **116**, 14–21 (2018). https://doi.org/10.1016/j.psep.2018.01.009
37. R.M. Khafagy, Synthesis, characterization, magnetic and electrical properties of the novel conductive and magnetic polyaniline/$MgFe_2O_4$ nanocomposite having the core-shell structure. J. Alloys Compd. **509**, 9849–9857 (2011). https://doi.org/10.1016/j.jallcom.2011.07.008

38. M.H. Beyki, H. Alijani, Y. Fazli, Optimization using response surface methodology for fast removal of hazardous azo dye by γ-Fe_2O_3@CuO nanohybrid synthesized by sol–gel combustion. Res. Chem. Intermed. **43**, 6245–6257 (2017). https://doi.org/10.1007/s11164-017-2987-3
39. T.R. Bastami, M.H. Entezari, Sono-synthesis of Mn_3O_4 nanoparticles in different media without additives. Chem. Eng. J. **164**, 261–266 (2010). https://doi.org/10.1016/j.cej.2010.08.030
40. F. Shirkavand, M. Hossein, F. Shemirani, Enhanced naproxen removal over magnetic quaternized dextrin ionomer: response surface optimization, kinetics, isotherm and comparing study. Desal. Water Treatm. **23324**, 1–19 (2018). https://doi.org/10.5004/dwt.2018.23324
41. G.R. Chaudhary, P. Bansal, S.K. Mehta, Recyclable CuS quantum dots as heterogeneous catalyst for Biginelli reaction under solvent free conditions. Chem. Eng. J. **243**, 217–224 (2014). https://doi.org/10.1016/j.cej.2014.01.012
42. C. Deng, X. Ge, H. Hu, L. Yao, C. Han, D. Zhao, Template-free and green sonochemical synthesis of hierarchically structured CuS hollow microspheres displaying excellent Fenton-like catalytic activities. CrystEngComm **16**, 2738–2745 (2014). https://doi.org/10.1039/C3CE42376J
43. K.A. Kumar, A. Pandurangan, S. Arumugam, M. Sathiskumar, Effect of Bi-functional hierarchical flower-like CoS nanostructure on its interfacial charge transport kinetics, magnetic and electrochemical behaviors for supercapacitor and DSSC applications. Sci. Rep. **9**, 1–16 (2019). https://doi.org/10.1038/s41598-018-37463-0
44. X. Liu, Z. Lei, F. Liu, D. Liu, Z. Wang, Fabricating three-dimensional carbohydrate hydrogel microarray for lectin-mediated bacterium capturing. Biosensors Bioelectron. **58**, 92–100 (2014). https://doi.org/10.1016/j.bios.2014.02.056
45. N. Tumin, A. Chuah, Adsorption of copper from aqueous solution by Elais Guineensis kernel activated carbon. J. Eng. Sci. Technol. **3**, 180–189 (2008)
46. M. Horká, F. Růžička, V. Holá, K. Šlais, Capillary isoelectric focusing of microorganisms in the pH range 2-5 in a dynamically modified FS capillary with UV detection. Anal. Bioanal. Chem. **385**, 840–846 (2006). https://doi.org/10.1007/s00216-006-0508-0
47. A. Denis, A. Touhami, Y.F. Dufre, Probing microbial cell surface charges by atomic force microscopy. Langmuir **18**, 9937–9941 (2002). https://doi.org/10.1021/la026273k
48. S. Rezaei-Zarchi, S. Imani, A.M. Zand, M. Saadati, Z. Zaghari, Study of bactericidal properties of carbohydrate-stabilized platinum oxide nanoparticles. Int. Nano Lett. **2**, 21–26 (2012). https://doi.org/10.1186/2228-5326-2-21
49. X.X. Sheng, Y.P. Ting, S.O. Pehkonen, The influence of ionic strength, nutrients and pH on bacterial adhesion to metals. J. Colloid Interf. Sci. **321**, 256–264 (2008). https://doi.org/10.1016/j.jcis.2008.02.038
50. M.C. van Loosdrecht, J. Lyklema, W. Norde, G. Schraa, A.J. Zehnder, The role of bacterial cell wall hydrophobicity in adhesion. Appl. Environ. Microbiol. **53**, 1893–1897 (1987). https://doi.org/10.1128/AEM.53.8.1893-1897.1987.
51. S. Shankar, R. Pangeni, J. Woo, J. Rhim, Preparation of sulfur nanoparticles and their antibacterial activity and cytotoxic effect. Mater. Sci. Eng. C **92**, 508–517 (2018). https://doi.org/10.1016/j.msec.2018.07.015
52. L. Wang, S. Xu, J. Li, Effects of phosphate on the transport of Escherichia coli O157:H7 in saturated quartz sand. Environ. Sci. Technol. **45**, 9566–9573 (2011). https://doi.org/10.1021/es201132s